Journal of Techniques, ISSN: 2708-8383, Vol. 5, No. 3, 2023, Pages 158-173
DOI: https://doi.org/10.51173/jt.v5i3.1469

JOURNAL OF TECHNIQUES

Journal homepage: http://journal.mtu.edu.iq

REVIEW ARTICLE - ENGINEERING

Lung Diseases Diagnosis-Based Deep Learning Methods: A Review

Shahad A. Salih[1*], Sadik Kamel Gharghan[1], Jinan F. Mahdi[1], Inas Jawad Kadhim[1]

[1] Electrical Engineering Technical College, Middle Technical University, Baghdad, Iraq

[*] Corresponding author E-mail: bdc0039@mtu.edu.iq

Article Info.

Article history:

Received
26 April 2023

Accepted
31 May 2023

Publishing
30 September 2023

Abstract

This review paper examines the current state of lung disease diagnosis based on deep learning (DL) methods. Lung diseases, such as Pneumonia, TB, Covid-19, and lung cancer, are significant causes of morbidity and mortality worldwide. Accurate and timely diagnosis of these diseases is essential for effective treatment and improved patient outcomes. DL methods, which utilize artificial neural networks to extract features from medical images automatically, have shown great promise in improving the accuracy and efficiency of lung disease diagnosis. This review discusses the various DL methods that have been developed for lung disease diagnosis, including convolutional neural networks (CNNs), deep neural networks (DNNs), and generative adversarial networks (GANs). The advantages and limitations of each method are discussed, along with the types of medical imaging techniques used, such as X-ray and computed tomography (CT). In addition, the review discusses the most commonly used performance metrics for evaluating the performance of DL for lung disease diagnosis: the area under the curve (AUC), sensitivity, specificity, F1-score, accuracy, precision, and the receiver operator characteristic curve (ROC). Moreover, the challenges and limitations of using DL for lung disease diagnosis, including the limited availability of annotated data, the variability in imaging techniques and disease presentation, and the interpretability and generalizability of DL models, are highlighted in this paper. Furthermore, strategies to overcome these challenges, such as transfer learning, data augmentation, and explainable AI, are also discussed. The review concludes with a call for further research to address the remaining challenges and realize DL's full potential for improving lung disease diagnosis and treatment.

Publisher: Middle Technical University

Keywords: COVID-19; CT Scan; Deep Learning; Image Processing; Lung Cancer; Pneumonia; Tuberculosis.

1. Introduction

In affluent countries, the superiority of the spread of chronic disease has increased continuously because of prominent risk factors, according to the 2017 GBD. Coronavirus Disease 2019 (COVID-19), Pneumonia, and tuberculosis (TB) are examples of lung diseases. Every year, an estimated 334 million cases of asthma lead to fatalities, while TB results in the death of 1.4 million people, and 1.6 million people die from lung cancer. Additionally, pneumonia claims the lives of millions of people. According to the Forum of International Respiratory Societies [1], there is a high healthcare burden, and many people are infected [2]. Fig. 1 shows the statistics of the world health organization (WHO) for lung diseases of the respiratory system [3].

In today's world and according to the tremendous rate of death causes and disability, it can be shown clearly how lung disease is a leading cause in those statistics. Detecting a disease in its early stages can significantly increase the likelihood of recovery and long-term survival [4]. Computer-Aided-Detection (CAD) systems for automatic pulmonary nodule detection were developed in the last two decades. The CAD system development is to fasten the interpretation of the CT images faster and more accurately, improving the screening program's cost-effectiveness [5]. Without the gained ability for deep learning (DL) to learn features from data, those developments could not occur compared to the features made by hand relying on specialized knowledge in a particular domain. In present times, DL is increasingly being recognized as a means of advancing performance in various medical applications, as shown in Fig. 2. Using medical images to diagnose lung diseases using one of the DL models. Those developments enhanced clinicians' efficiency in examining and detecting certain medical cases [6]. Technology development has ushered in a new era with challenges and possibilities. Technology, especially Artificial Intelligence (AI) [8], is vital in almost industry. They do this with the help of intelligent algorithms and powerful computers. However, each business is very different in how much it depends on computers. Technology is now an essential part of healthcare and medicine. It is possible by automating tasks and processes people used to do by hand. It saves time and makes it easier to understand diseases that are hard to explain. It could also decrease the cost of healthcare as a whole. In the past few decades, radiologists and physicians did most of the work of figuring out what medical images meant. Nevertheless, because so many diseases and experts can get tired, researchers and doctors are starting to use computer-assisted interventions [9]. Learning from data is frequently utilized in CAD and examining medical images. In the realm of AI (i.e. machine learning), the classification process typically involves a sequence of procedures, including but not limited to feature extraction, learning, pre-processing, highly accurate feature selection, and classification. These steps are considered fundamental in traditional ML methodologies. The main thing used to make a choice is the chosen feature. However, it is possible that these things can be wrong and cannot be relied on to tell classes apart. Machines. DL helps the researcher to get features and classify them all at once.

Nomenclature & Symbols

AI	Artificial Intelligence	ANN	Artificial Neural Network
AUC	Area Under the Curve	CAD	Computer Aided Detection
CAP	Community Acquired Pneumonia	CNN	Convolutional Neural Network
CT	Computed Tomography	DCNN	Deep Convolutional Neural Network
DL	Deep Learning	DNN	Deep Neural Network
DT	Decision Tree	DWT	Discrete Wavelet Transform
EBT	Bagged Tree	FN	False Negative
FP	False Positive	GANs	Generative Adversarial Network
GLGCM	Gray Level Gradient Co-Occurrence Matrix	GLRLM	Gray Level Run Length Matrix
GLSZM	Gray Level Size Zone Matrix	GP	General Pneumonia
HOG	Histogram Oriented Gradient	KNN	K Nearest Neighbor
LBP	Local Binary Pattern	LDP	Local Directional Patter
LSTM	Long Short Term Memory	MFCC	Mel-Frequency Cepstral Coefficients
ML	Machine Learning	MSCNN	Multi Scale Convolutional Neural Network
PNN	Probabilistic Neural Network	RNN	Recurrent Neural Network
ROC	Receiver Operator Characteristic Curve	ROI	Region of Interest
SVM	Support Vector Machine	TB	Tuberculosis
TL	Transfer Learning	TN	True Negative
VGG 16	Visual Geometry Group 16	WHO	World Health Organization

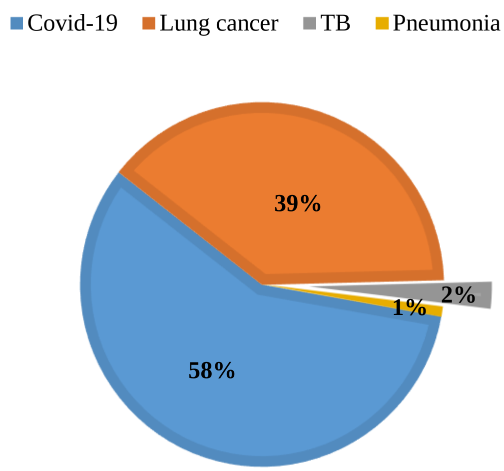

Fig. 1. Most commonly used datasets in previous articles for lung diseases

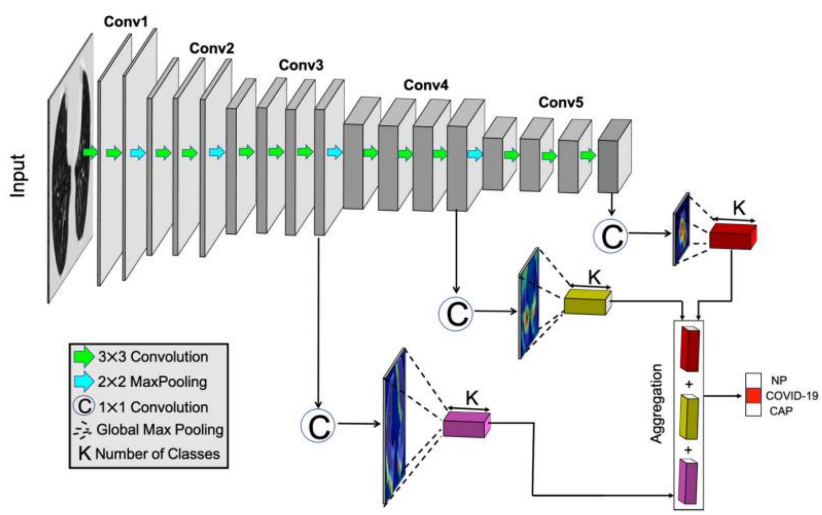

Fig. 2. CT images detect diagnosing lung diseases using the convolutional neural networks (CNN) model [7]

With the advent of Machine Learning (ML) and DL techniques [10], DL utilizing Artificial Neural Networks has emerged as one of the most vital feature extraction and diagnosis techniques. Despite multiple ML techniques for analyzing medical images in various domains, DL has emerged as the superior approach to looking at and understanding medical problems because it is more accurate [11]. DL is a subset of ML that utilizes Deep Neural Networks (DNNs) with multiple inputs, outputs, and hidden layers. DL has gained widespread recognition for its applications in various domains. Still, it is essential to analyze and interpret medical images to get around the limitations of image processing and ML methods, which is apparent in Fig. 3. However, these uses of DL are not very good at classifying things because there is not enough training data, and the models are not built well. DL models need data to work well [12]. Note that the inadequate training data makes DL model network training inefficient. Before medical imaging uses CAD, these issues must be resolved.

The remaining sections of the paper are structured as follows: Section 2 discusses the types of lung disease images utilized in this research, while Section 3 presents the specific type of lung disease images examined in this study. Section 4 explains the process of image feature extraction using image processing and DL technique models, with a brief explanation of each model. In Section 5, previous works in this area are presented and compared. Section 6 introduces the mathematical models used to evaluate performance metrics for diagnosing lung diseases. Finally, Section 7 highlights the advantages of DL algorithms in diagnosing lung diseases. In Section 8, the challenges and limitations associated with the diagnosis of lung diseases are presented. Finally, the paper concludes in Section 9.

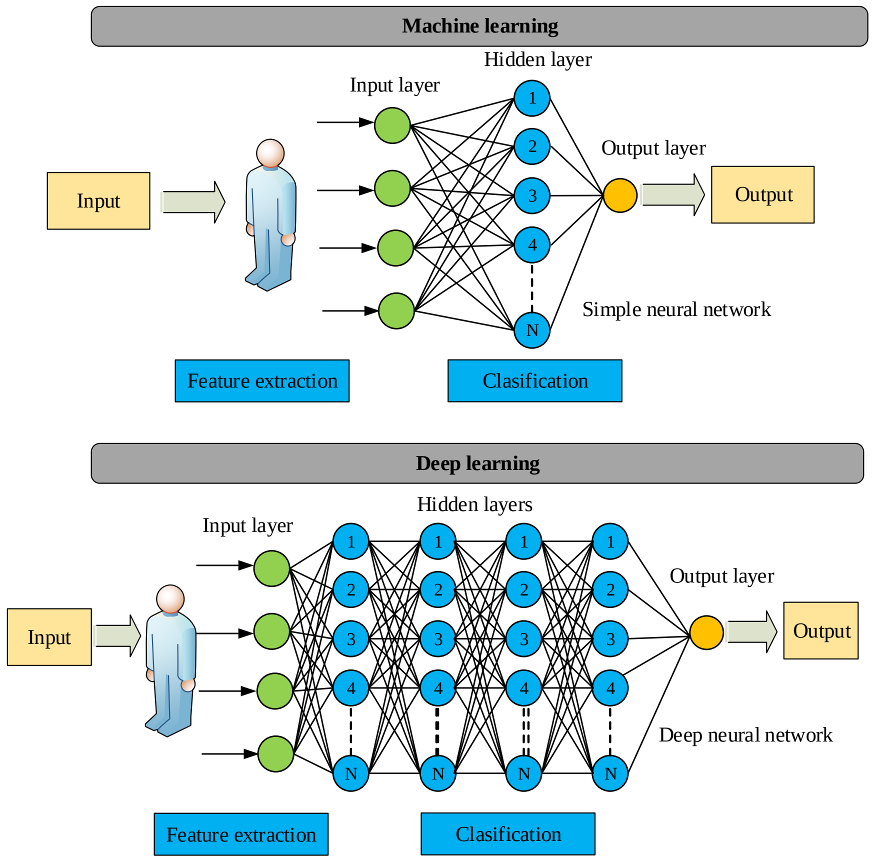

Fig. 3. Difference between deep and traditional ML

2. Type of Lung Disease

This section will briefly discuss the four diseases affecting the respiratory system and the lung, such as COVID-19, TB, Pneumonia and lung cancer.

2.1. COVID-19

Since December 2019, a new coronavirus illness has emerged, COVID-19 or 2019-nCoV. COVID-19 causes severe respiratory symptoms and widespread damage to the respiratory system. Coronavirus transmission can be reduced like any other illness, and patient survival rates can be improved via prompt identification and treatment. The clinician's go-to method for determining whether or not COVID-19 is present is the RT-PCR. According to the medical community, this method's positive rate is modest in the preliminary stages of this condition. As a result, physicians have to turn to another method to aid in rapidly identifying COVID-2019. As a result, the doctor looks more closely at the patient's CT scans and chest X-rays. Both techniques demonstrate that COVID-19 causes a unique lung alteration compared to other pneumonic diseases. Different AI algorithms and combinations of these algorithms are used to categorize these images. The results are contrasted and compared to ascertain the most effective approach, such as convolutional neural networks (CNN), k-nearest neighbor (k-NN), and Random Forest.

2.2. TB

TB has been a persistent problem among all infectious diseases, resulting in considerable morbidity and mortality. It makes TB more challenging to treat than other infectious diseases. Following a consistent decline in the number of new TB cases during the twentieth century, owing to improved social and environmental conditions, early detection, and the development of medication for treatment, stagnation and even a surge in new cases were observed in the mid-1980s. Improved social and environmental conditions, early detection, and the development of medication specifically for TB[13]. Were the key factors contributing to the decrease in the number of new TB cases. The epidemiological shift can be attributed to a combination of factors, including an overall rise in developing nations, an increase in the number of people living with

HIV and other forms of immunodeficiency, and an increase in the number of elderly patients whose immune systems have changed. Incomplete or insufficient treatment, the growth of multidrug-resistant TB, and a delayed diagnosis are other reasons that may be to fault. A delayed diagnosis is more common in people over the age of 65. The interaction between the organism and the host response determines the disease's progression and associated clinical and radiological patterns. Both of these aspects are dependent on each other. In the past, pulmonary TB was traditionally divided into two categories: primary TB, which affected children and post-primary TB, which affected adult patients. Primary TB was more common. However, adults, rather than children, were becoming infected with TB for the first time in developed nations[14].

2.3. Pneumonia

Pneumonia is a common lung illness in which a person's alveoli fill up with fluid and create a cloudy-like shape. It happens when a person has Pneumonia. There are two different kinds of Pneumonia, bacterial and viral, yet the X-ray patterns of each look highly similar[15]. That requires guidance from computer-aided diagnostic tools. DL technology was utilized to diagnose Pneumonia in this investigation. Training the models, such as the VGG16 and Xception network, to better detect pneumonia cases. Thus, every network has unique capabilities to detect these diseases [16].

2.4. Lung cancer

Diagnostic imaging has shown lung nodules. Before CT scanning, chest X-ray lesions typically required resection. These tiny tumours (less than 3 cm) can cause symptoms such as sneezing, post-obstructive pneumonia, and hemoptysis. A lack of symptoms and solitary nodules in the lungs may also be present if they originate in the lung parenchyma. Lung nodules can be caused by several conditions besides malignant tumours[17]. Doctors' experience diagnosing lung cancer may overlook some individuals and cause issues. Medical imaging diagnosis uses DL. This article designs CNN, DNN, and sparse auto-encoder deep neural networks for lung cancer calcification. Those networks are modified for benign and malignant lung nodules and used for CT image categorization [18].

3. Lung Diseases Image Type

Two distinct types of images are employed in training the model: CT-Scans and X-rays. These images are described in detail in Section 2. It is important to remember that additional imaging modalities, such as MRI scans, positron emission tomography, histopathology images, and sputum smear microscopy images, are all available. PET and MRI scans can detect disease and monitor treatment results. Unfortunately, only CT scans and X-rays are used in this review paper.

3.1. Lung diseases- based chest X-rays

X-rays are a standard diagnostic tool used by doctors to understand better and treat various health issues [19]. A chest X-ray is the most common type of medical X-ray examination, and the resulting pictures may be used to examine organs like the heart, lungs, and airways, as well as the vertebrae and ribs in the patient's chest. Images captured by medical X-rays were previously subjected to photographic films, which must be developed before they can be seen. Digital X-rays are utilized to get around this issue [20]. Fig. 4 shows medical images of patients with various lung diseases based on X-rays.

(a) (b) (c) (d) (e)

Fig.4. Shows a collection of x-ray images; (a)normal condition [21], (b) tubercles condition [22], (c) Lung cancer condition [23], (d) Pneumonia condition [21], and (e) COVID-19 condition [24]

3.2. Lung diseases- based CT Scans

Radiography in a CT scan employs a series of pictures collected from different angles to construct cross-sectional pictures at different depths[25]. The patient's tissues, organs, skeleton, and any anomalies can be shown in 2D on a flat screen or 3D by stacking the picture slices[18]. When compared to X-rays, CT scan pictures provide more information. Fig. 5 illustrates some CT scans images used to detect lung diseases.

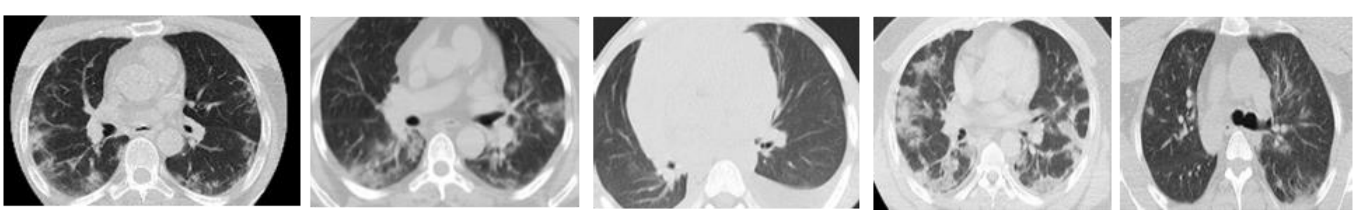

(a) (b) (c) (d) (e)

Fig. 5. Shows a collection of CT Scans images; (a) normal condition [26], (b) tubercles condition [27], (c) Lung cancer condition [28], (d) Lung cancer condition, (e) COVID-19 condition [29]

4. Feature-Extraction

In order to perform a target task, it is commonly done to utilize a previously trained CNN model that has been trained on a large dataset. To accomplish this, it is necessary to preserve all model layers and adapt those fully connected to correspond with the new task. Convolutional layers are used to extract the feature. The information is then sent to a classifier built from fully connected layers and may be swapped out for a different job, or one of the ML classifiers, such as k-NN, support vector machine (SVM), etc., can be utilized. Instead of retraining the whole model, just the new classifier is trained [30]. The key benefit of this strategy is the time savings gained by not having to re-run the model during each training iteration but rather only once on the new data. However, updating the training data on all is impossible with this method. Fig. 6 shows that convolution, pooling, and fully connected layers are essential elements of the CNN model. Sections 4.1 through 4.4 summarize the pre-trained models employed in this analysis.

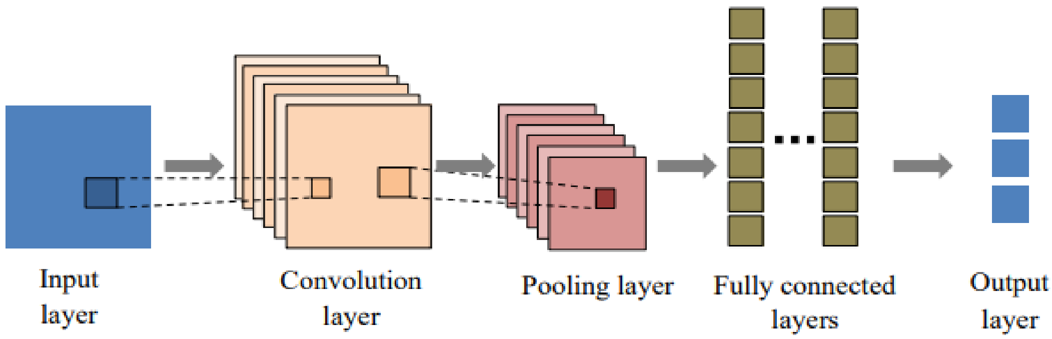

Fig. 6. Example of CNN architecture [31]

4.1. VGG16

The Visual Geometry Group 16 (VGG16) model was submitted to the Large Scale Visual Recognition Challenge 2014 (ILSVRC2014) [32]. VGG16 is a convolutional neural network (CNN) model with 16 layers, including 13 convolutional layers and three fully connected layers. The Visual Geometry Group developed it at the University of Oxford and has achieved state-of-the-art performance on various computer vision tasks, including image classification and object detection. The VGG16 model is widely used in DL research and has become a benchmark for comparing the performance of other CNN models [33]. The VGG16 model architecture contains over 138 million weights. An illustration of the VGG16 model architecture is presented in Fig. 7.

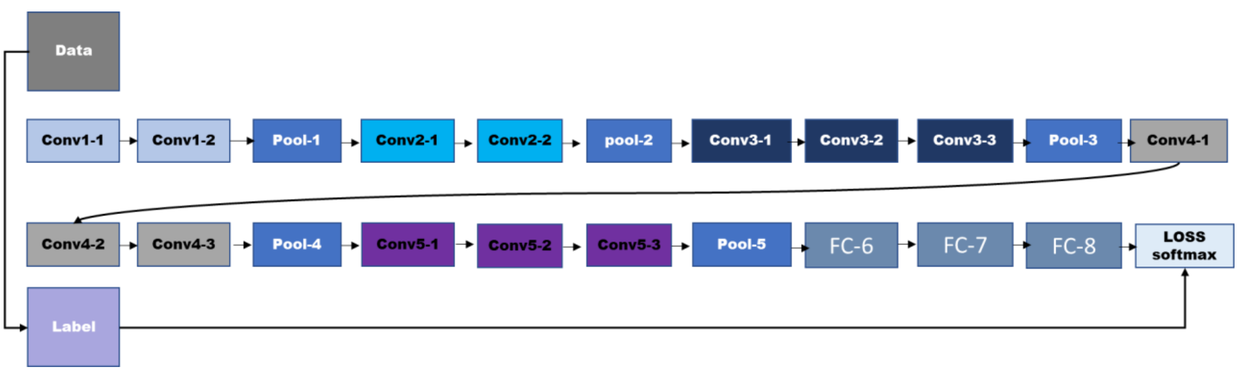

Fig. 7. VGG16 model architecture [34]

4.2. Xception

The Xception model was suggested in 2017 [35]. Xception is a modified version of the Inception-V3 model, and it is named Extreme Inception. The Xception framework's CNN model consists of 36 convolutional layers grouped into 14 components. In contrast, the Xception model has a 134-layer architecture. It can handle 22.9 million inputs. The first two layers of Xception are standard convolutional layers with 32 and 64 filters with a 3x3 filter size. The following five blocks are Exceptions. With the exception of the last Xception block, each input undergoes two separate convolutional layers, a max-pooling layer and a pointwise convolution through a shortcut link. Eight copies of the fourth Xception block, comprising a single disconnected convolutional layer, generate the final output. A global average pooling layer comes after the final Xception block, with two independent convolutional layers. The last layer is the output layer, inserted after all the ultimately linked layers [36]. Fig. 8 illustrates the architecture of the Xception deep CNN model.

4.3. MobileNetv2

Since its inception, MobileNet has undergone two major revisions, V1 and V2. The newer MobilenetV2 is a vast improvement over its predecessor [38]. The MobileNet design is based on a typical convolution split into a depth-wise convolution and a 1x1 convolution, known as a pointwise convolution. Each input channel undergoes a single filter application in the depth-wise convolution. An 11 convolution is applied in the pointwise convolution to integrate the results of the depth-wise convolution.

In contrast to the one-step process of a conventional convolution, which involves mixing the inputs and filters to generate a new set of outputs, the depth-wise version of the algorithm separates these processes into separate layers. Reduced model size and calculation time are two significant benefits of this approach. Fig. 9 presents two DL models; MobileNet and MobileNetV2.

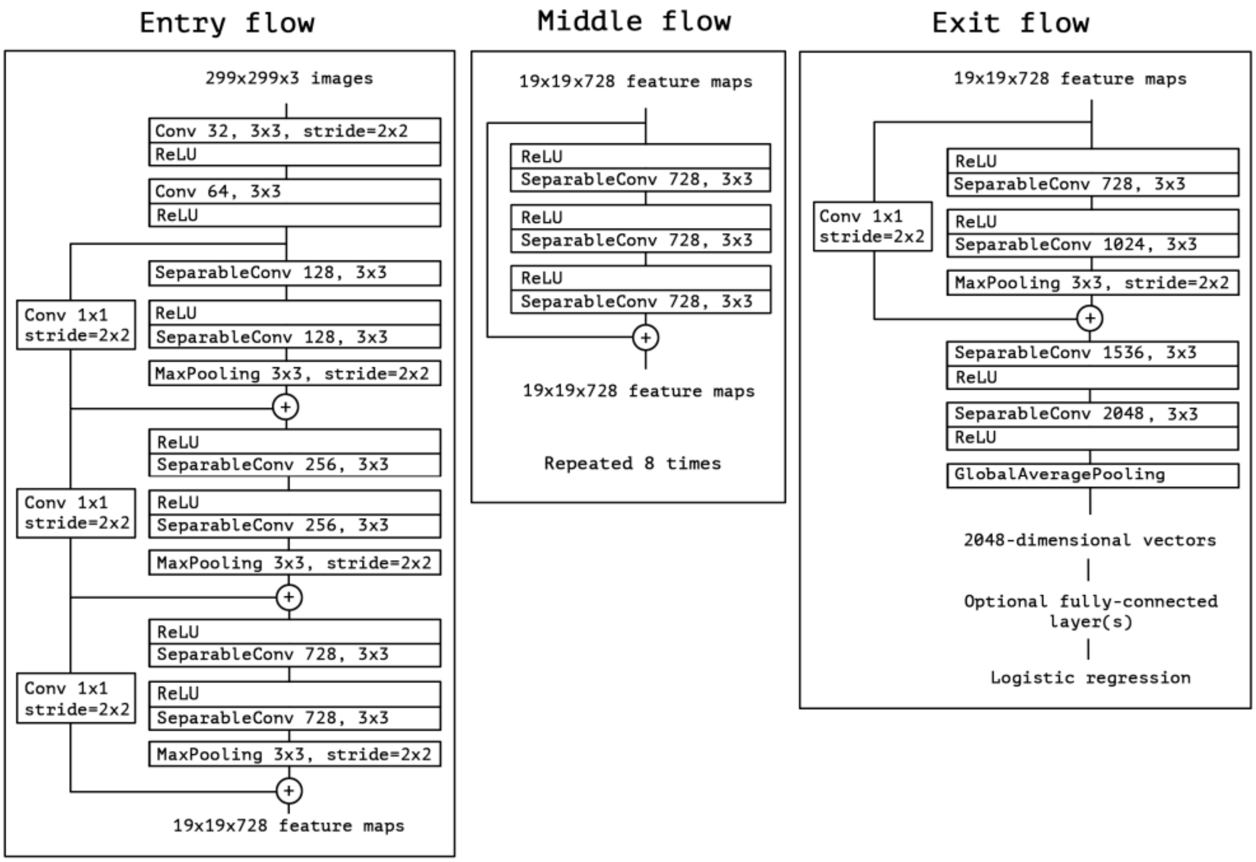

Fig. 8. The architecture of the Xception deep CNN model [37]

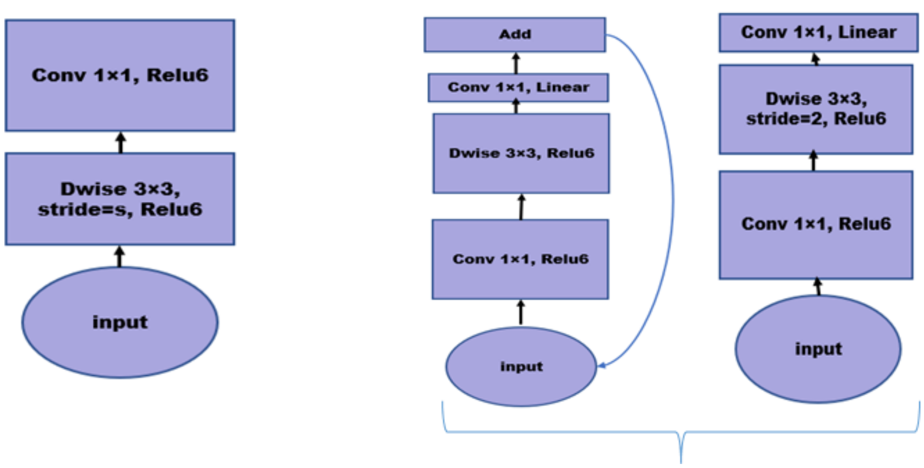

(a) (b)

Fig. 9. DL models; (a) MobileNet and (b) MobileNetV2 [39]

4.4. ResNet50

In 2015, ResNet won the ILSVRC competition [138]. ResNet50 is a 50-layer CNN. ResNet, which stands for Residual Networks, is a time-tested neural network that is the backbone of many computer vision applications [139]. With ResNet, a deep network might address the vanished scales that affected earlier networks and can be created when accuracy reaches a plateau at a specific size and then rapidly declines due to decreasing gradient values. ResNet uses residual blocks to address this issue by using shortcut connections across layers, each consisting of convolutional, RELU, and batch normalization layers. The outputs of the stacked layers are combined with the outputs of the shortcut connections, which carry out identity mapping. One-to-one, three-to-three, and one-to-one convolutions make up the three convolutional layers. The 11 layers compress the dimensions and then expand them (restore them). After the residual block has been established, intense networks may be constructed by stacking them [140]. The ResNet-50 model handles 25.6 million parameters, improving accuracy without increasing network depth and protecting against corruption as the CNN increases. Fig. 10 introduces an example of the detection of covid-19 using a deep-learning model named ResNet50.

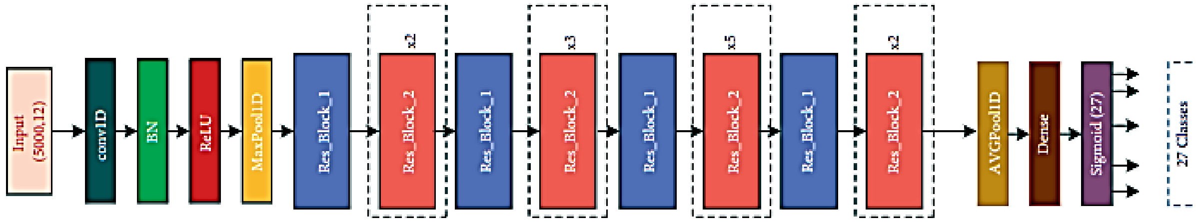

Fig. 10 The architecture of the ResNet-50 model [40]

5. Previous Work

Based on clinical pictures, many ML and DL-based models have been built to identify lung disorders (CT scans and X-rays of the chest). When creating the methodology for this study, it is crucial to consider the most current research conducted in this area, which is discussed in the following review.

5.1. X-ray-based DL techniques

Rajaraman et al. [41] investigated an enhancing technique to improve the detection performance of TB lung diseases with a chest X-ray dataset that was divided into four sections (S, M, K, and I) by using CNN based on classifier models AlexNet, VGG16, GoogleNET and ResNet50. The findings were convincing and surpassed the existing cutting-edge. Ayan and Ünver [16] examined a new diagnostic technique for one of the most severe human lung infections, Pneumonia, using two commonly used CNN models. The network can provide clear X-ray images that radiologists can use as a successful diagnosis of the disease. The research used a data sample of 5856 frontal chest X-ray pictures and introduced them to two computerized support systems named VGG16 and Xception, which showed remarkable results in image classification. However, transfer learning and fine-tuning techniques were employed to train the two CNNs. The test outcomes have demonstrated that the VGG16 neural network far exceeds the Xception model in accuracy by 87%, pneumonia precision by 91%, specificity by 91%, and pneumonia F1 score by 90%. At the same time, the Xception network transcends the VGG16 network with regular precision of 86%, a sensitivity of 85%, and a pneumonia recall of 94%. The test result has shown that the VGG16 network is more accurate in the data than the Xception, but the Xception provided more successful results in detecting pneumonia cases.

Capizzi et al. [42] designed a special detection technique for lung cancer by using a probabilistic neural network (PNN) with fuzzy logic. This study used X-ray images of lung nodules to verify our model by computing the local variance on each pixel. Moreover, the suggested approach identifies and localizes possibly hazardous lung nodules. Finally, the test result has produced excellent outcomes compared to other models. Hou and Gwak [43] designed an automatic screening competitive technique for lung abnormalities images using a classified DL technique named knowledge distillation. The study used a dataset from the public ChestX-ray14 of thorax diseases. This strategy was designed to condense information from heavyweight teacher models such as ResNet-152 and DenseNet-121into lightweight student models such as MobileNet, VGG19, ResNet-59, and ResNet-50 or to self-train these student models in order to obtain poorly supervised multi-label lung disease diagnoses.

Tobias et al. [44] created a low-cost screening tool to classify normal or Pneumonia using a DL technique called CNN. The dataset used was chest X-rays of 6,555 images divided into 1,340 images of normal lung and 5215 images of Pneumonia. It presented them with a pre-trained model named MobileNetV2 that produced excellent results. Gite et al. [45] developed a new advanced segmentation technology to decrease the possibility of data leakage in diagnosing TB diseases by using DL instead of the classification architecture to focus on the vital region of the chest X-ray lung images, using U-Net + + and comparing them with neural network architecture such as SegNet, U-Net, and FCN. The generated result was tested on Shenzhen and Montgomery databases that showed U-Net + + achieved 98% accuracy; this indicates that it exceeds other architecture. Bhosale et al. [46] developed advanced IoT to reduce mortality and detect covid-19 and other obstructive lung diseases using a lightweight DL single model CNN technique using different chest X-ray images. The results showed encouraging output and enabled raspberry pi to detect lung disease. Table 1 compares the abovementioned research using X-ray-based DL techniques for lung disease recognition.

Table 1. Comparison of research using X-ray-based DL techniques for lung disease detection

Ref/ year	Algorithm	Model	Type of diseases	Performance matrices						
				Accuracy (%)	Sensitivity (%)	Specificity (%)	F1-score (%)	Precision (%)	ROC (%)	AUC (%)
[41]/ 2018	CNN	AlexNet , VGG-16 , GoogLe –Net, and ResNet-50	TB	Best result achieved By AlexNet: 0.872	-----	-----	-----	-----	-----	Best result achieved By AlexNet: 0.950
[47]/2019	CNN	VGG-16	pneumonia	0.82	0.85	0.76	0.87	0.82	0.94	-----
		Xception		0.87	0.82	0.91	0.90	0.91	0.89	-----
[42]/2019	PNN	Fuzzy-Logic	lung cancer	92.56	0.95	0.90	-----	-----	-----	-----

[43]/2020	CNN	MobilNet VGG-19 ResNet-32 ResNet-50 DenceNet	lung abnormalities		-----	-----	-----	-----	-----	0.671 0.7617 0.6605 0.7166 0.8097
[44]/2020	CNN	Mobile-NetV2	Pneumonia	99.8408	-----	-----	-----	-----	-----	-----
[46]/2022	CNN	LDC-Net	Covid-19	99.28	-----	-----	96.77	96.86	96.78	-----
[45]/2022	DNN	U-Net + +	TB	98	0.0148	0.0344	-----	0.0688	0.014	-----

5.2. CT-scan-based DL techniques

Wang et al. [48] designed a segmentation and early diagnosis technique for lung cancer using CAD and two CNN models. The study used a big-driven dataset of CT images and exported them to two models named AlexNet and ResNet that were used to train and test the data experiment. The training results displayed that AlexNet had high experimented than ResNet with an accuracy of 76% of AlexNet and 58% of ResNet. The advantage of this technique is that it can be used in pulmonary nodule extraction and automated recognition, which may save numerous lives. Still, it can also help to relieve medical resources, doctors, and patients. Yadav et al. [49] proposed an unsupervised DL system to diagnose lung disorders with chest X-ray and CT scans classification, such as Pneumonia and covid-19, by using a stacking classifier model that includes The model was trained by using a multi-layer GAN architecture called Lung- generative adversarial networks (GANs) the result achieved an excellent accuracy, precision, recall, F1-score. Tang et al. [50] developed a study of the segmentation of lung lob through the implementation of trained neurons, specifically DCNN. The study presented a dataset of 50 axial, sagittal, and coronal CT scans to LUNA16 and Tranche. The DL model was trained with dice loss, and the focal loss model and the convex hull model were trained with hybrid loss.

Hu et al. [51] presented a weak supervised DL system CNN for rapid and automated diagnosis with data analysis. One of the diseases that might lead to death is COVID-19 infection using CT images from Community-acquired Pneumonia (CAP) and non-pneumonia clients. This system worked with a model that trained segmentation such as cross-validated and tested with actual manual truth TCIA dataset. Ardakani et al. [52] utilized several DL models to distinguish between patients with and without COVID-19. These networks were AlexNet, ResNet-18, VGG-19, GoogleNet, ResNet-101SqueezeNet, MobileNet-V2, ResNet-50, VGG-16 and Xception. This research comprised 108 individuals with COVID-19-positive lab results. In addition, 86 cases with atypical pneumonia were included. Their work adopted transfer learning to optimize CNNs for the datasets. The CNNs' input layer was a 60 x 60 x 1 infection patch, where 1020 image patches, including 510 COVID-19 and 510 Non-COVID-19, were extracted from CT slices by a radiologist specializing in infectious diseases. The findings indicated that ResNet-101 and Xception performed the best job among the ten networks. ResNet-101 could differentiate between COVID-19 and non-COVID-19 patients.

Hasan et al. [53] designed algorithms to distinguish chest CT scans between three classes (COVID-19, Pneumonia, and healthy) using a combination of DL and handmade Q-deformed entropy (Q-DE) algorithms for extracting features. The pictures are pre-processed for the purpose of decreasing intensity differences across CT slices, and the CT lung scan was segmented using the histogram threshold. A recurrent neural network (RNN) based on long-short-term memory (LSTM), along with CNN and the Q-DE method, was used to classify the features extracted from each CT scan. In addition, an examination of variance ANOVA was employed to identify the pertinent characteristics. The data samples comprised 118 CT scans images of COVID-19 patients, 107 healthy people, and 96 pneumonia patients. The suggested paradigm achieved a 99.68% classification rate.

Pathak et al. [54] used Transfer Learning (TL) on the pre-trained network to create a COVID-19 classification model using 10-fold cross-validation to avoid overfitting. A ResNet-50 network extracted chest CT image characteristics in the primary model design. Transfer learning was used to modify the deep layer starting parameters for the classification model. In addition, a CNN model consisting of a Softmax layer and four convolutional layers for activation was employed for classification. 413 COVID-19 and 439 are regular or pneumonia-infected CT scans were utilized. The training accuracy of data was found to be 96.2%, while the accuracy of testing data was 93%. Yan et al. [55] created a classification system employing a multi-scale convolutional neural network (MSCNN) and tested its impact on slice and scan diagnosis. To better classify multi-scale input pictures (128x128, 256x256, and 512x512), the MSCNN architecture learned feature representations. EfficientNetB0, a pre-trained network, was the backbone of three CNNs with the same structure but varied input scales for feature extraction. A dense, fully connected classifier with a sigmoid output activation function classified Hospitals provided 416 COVID-19 CT scans and 412 CAP CT scans. The system has 99.5% slice sensitivity and 95.6% slice specificity.

Liu et al. [56] presented a methodology to distinguish COVID-19 from general pneumonia (GP) patients based on statistics and ML classifiers. Ground-glass opacities defined the region of Interest (ROI) manually. The COVID-19 and GP pictures extracted 34 statistical texture features, including 15 Gray Level Gradient Co-occurrence Matrix (GLGCM) features, 13 GLCM features, and six histogram features. Then, a feature selection approach (the RelieFF algorithm) optimized classification. Finally, five feature sets were chosen. The ideal features set and the other four combinations were examined using ten folds of cross-validation to assess five classification techniques: the ensemble of the SVM, the bagged tree (EBT), the logistic regression (LR), the decision tree (DT), and the K-NN. A hospital gathered 73 COVID-19 CT scans and 27 general pneumonitis CT images. The EBT technique had 94.16% classification accuracy, 88.62% sensitivity, and 100.00% specificity, which was more consistent than other classifiers.

Li et al. [57] created a 3D DL technique, COVNet, to identify COVID-19 using 2D and 3D characteristics. U-Net neural network pre-processed the 3D CT scan to delineate the ROI. The COVNet, consisting of RestNet50, which forms the framework, collected features from a series of CT slices and performed a max-pooling operation to merge these features. A fully linked layer classifies in-depth features using the softmax activation function. COVID-19, CAP, and non-pneumonia were identified. The dataset contained 1292 COVID-19, 1735 CAP, and 1325 non-pneumonia CT images. Additionally, the authors employed Gradient-Weighted-Class Activation Mapping to visualize important regions identified by the model without any human annotation. The model detected COVID-19 with 90% sensitivity and 96% specificity. Wang et al. [58] used a lightly supervised DL system to identify COVID-19 from CT scan pictures without lesion annotation. The lung area was partitioned using a pre-trained U-Net, providing a 3D lung mask to a 3D DNN that predicted COVID-19 infection. 313 COVID-19 and 229 non-COVID-19 patients were studied. DeCoVNet was a three-stage model with two 3D residual blocks (ResBlocks), vanilla 3D convolution to extract image features, and a progressive classifier (three 3D convolutional layers, a fully connected layer, and a softmax activation function). The algorithm has 90.1% classification accuracy.

Toqa et al. [59] developed a novel CNN for image classification, explicitly targeting the CT scans of COVID-19 patients. The model was trained and evaluated using 349 patients with COVID-19 photos and 195 without COVID-19 images. Augmentation of data was also employed to deal with the limited amount of the data samples. The suggested model used the softmax activation function at the output layer and had four convolutional blocks. Validation accuracy was 84.4%, while testing accuracy was 90.09% for this model. Compared to other pre-trained CNNs, the suggested model's performance confirmed its superiority in detecting capabilities (ResNet-50 and AlexNet). Adil et al. [47] developed the Deep Sense technique, a cross between a recurrent gated unit GRU neural network and a CNN. The model used three independent convolutional subnets to extract picture features, a merged convolutional subnet to process that output, and a GRU and output layer stacked in an 8-layer deep network to do classification. This model was tested on three distinct CT image benchmark datasets with varying validation and test splits, and it was compared to two other models built using an ANN. Compared to competing models using alternative data, the suggested model was shown to perform better in testing.

Mucahid et al. [60] produced an ML COVID-19 classification scheme. It was divided into four subsets of differing sizes before being fed into the SVM classifier. To classify the four datasets, the author collected features by hand and fed them into (SVM), evaluating five different textural feature extraction methods. Several methods, including the Grey Level Co-Occurrence Matrix (GLCM), the Grey Level Run Length Matrix (GLRLM), the Grey-Level Size Zone Matrix (GLSZM), the Discrete Wavelet Transform (DWT), and the Local Directional Pattern Algorithm (LDP), were implemented. 150 CT images were used, and squares varying in size from 16 by 16 to 48 and 48 to 64 by 64 were selected randomly. The results showed that the GLSZM algorithm could achieve 98.71% accuracy using 5-fold cross-validation and a batch size of 100 (32 x 32). Shuai et al. [58] DL algorithm to filter CT images for COVID-19. A binary solution categorization is required for addressing both COVID-19 and typical pneumonia. The model's input photos were pre-processed to determine the ROI. The ROI was drawn from CT images using COVID-19 and viral pneumonia characteristics. Transfer learning was used to extract features from images using a modified Google-Net Inception v3 (M-Inception) network. This model extracted features that reduce ROI feature vector size. Categorization and prediction employ a fully connected network. One hundred eighty patients had typical viral Pneumonia, whereas 979 had COVID-19 (positive RT-PCR) and were treated at three facilities. The model was 89.5% accurate when internally validated but only 79.3% when externally validated.

Shah et al. [61] CT scans are automatically diagnosed and classed as normal or abnormal. As a result, clinicians rely on this approach to provide accurate and timely diagnoses, and these pictures are classified using DL models like the CTnet-10 model. It is due to the simplicity and speed with that it can be trained. However, the accuracy results are low compared to other models utilized, especially the VGG-19, where the results are 82.1% for the CTnet-10 and 94.52% for the VGG-19. Panwar et al. [62] used a transfer learning method to binary classify chest X-ray and CT scan images. The suggested technique used VGG-19 CNN pre-trained weights to assess in-depth features and incorporated five layers as a deep neural network classifier (a flat layer, two dense layers, average pooling, and a dropout layer). GradCAM used colour visualization to help radiologists understand the model. Chest X-ray and CT-scan images of four cases were included in the datasets: COVID-19, Non-COVID-19, Pneumonia, and Normal. CT scans included 1252 COVID-19 patients and 1230 non-COVID patients with other pulmonary disorders, while X-rays included 285 COVID-19 patients and 5856 pneumonia and regular patients. The model detected 95.61 percent of COVID-19 instances.

Luqy et al. [63] created three independent feature extraction techniques grey level co-occurrence matrix (GLCM), local binary pattern (LBP), and histogram-oriented gradient (HOG)were suggested to be combined. The authors applied principal component analysis on the output features generated by these techniques to decrease the number of features. The SVM is a machine-learning classifier used for classification. The data used to design the system (available on the online platform Kaggle) consists of 1100 CT scans and 1100 X-ray scans. The picture had 550 students in each class (with COVID-19 and no infected with COVID-19). When utilized with X-ray and CT scans pictures, the method provided an accuracy of 97% and 99%, respectively, for the binary categorization of COVID-19 and non-COVID-19. Table 2 compares the earlier research using CT scan-based DL techniques for lung disease identification.

Table 2. Comparison of previous research employing CT scan-based DL techniques for lung disease identification

Ref/year	Algorithm	Model	Type of diseases	Performance matrices						
				Accuracy (%)	Sensitivity (%)	Specificity (%)	F1 score (%)	Precision (%)	ROC (%)	AUC (%)
[48]/ 2017	CNN	AlexNet, ResNet	Pulmonary nodules	0.76 0.58	-----	-----	-----	-----	-----	-----
[50]/ 2019	CNN	LUNA16 Tianchi	pulmonary lobe segmentation	FL:90.94 ,92.25 DL:87.07 ,88.30 CH:91.48 ,94.17	-----	-----	-----	-----	-----	-----
[51]/ 2020	CNN	CNN	COVID-19, Community-Acquired Pneumonia (CAP)	81.0 74.8	80.2 76.3	82.6 71.1	-----	83.2 76.3	-----	0.816 0.792

[52]/ 2020	CNN	AlexNet, VGG-16, VGG-19, Squeeze-Net, Google-Net, Mobile-Net-V2, ResNet-18, ResNet-50, ResNet-101, and Xception	COVID-19	the best performance was achieved by ResNet-101: 99.51 and Xception: 99.02	ResNet-101: 100 and Xception: 98.04	ResNet-101: 99.02 and Xception: 100.	-----	-----	-----	For both: 0.994
[53]/ 2020	CNN	LSTM	COVID-19, pneumonia	99.68	-----	-----	-----	-----	-----	-----
[54]/ 2020	(TL)	ResNet-50	COVID-19	93	-----	-----	-----	-----	-----	-----
[55]/ 2020	CNN	MSCNN	COVID-19	87.5	89.1	85.7%	-----	-----	-----	0.934
[56]/ 2020	(ML)	EBT, DT, LR, K-NN, and SVM	COVID-19 and GP	EBT is more consistent than other classifiers achieved: 94.16.	88.62	100.	-----	-----	-----	-----
[57]/ 2020	U-Net	RestNet50	CAP COVID-19	-----	90	96.	-----	-----	-----	-----
[64] 2020	lightly supervise DL	DeCoV-Net	COVID-19	-----	90.1	-----	-----	-----	-----	-----
[62] /2020	CNN	VGG-19	COVID-19	95.61	-----	-----	-----	-----	-----	-----
[59]/ 2020	CNN	ResNet-50 and Alex Net	COVID-19	The model achieve an accuracy of 84. for validation anc 90.09 for testing.	-----	-----	-----	-----	-----	-----
[47]/ 2020	ML	FFNN	COVID-19	97.44	90.59	97.54	-----	-----	-----	-----
	ML	ANN		97.44	90.59	97.53	-----	-----	-----	-----
	ML	BPNN		97.52	91.40	97.63	-----	-----	-----	-----
	ML	DNN		97.52	91.53	97.63	-----	-----	-----	-----
	ML	RNN		97.54	92.27	97.72	-----	-----	-----	-----
	ML	DeepSense		97.59	92.34	97.72	-----	-----	-----	-----
[60]/ 2020	ML	GLCM GLRLM GLSZM DWT LDP	COVID-19	GLSZMachieved the best result: 99.68	-----	-----	-----	-----	-----	-----
[49]/ 2021	Lung-GANs	stacking classifier model, L2SVM	pneumonia and covid-19	94.0 to 99.5	-----	-----	0.94 to 1.00	0.93 to 1.00	0.93 to 1.00	-----
[58]/ 2021	Transfer learning	Google-Net	COVID-19	89.5	-----	-----	-----	-----	-----	-----
[63]/ 2021	ML	GLCM, LBP, and HOG.	COVID-19	97	-----	-----	-----	-----	-----	-----
[61]/ 2021	DL	CTnet-10, VGG-19	Lung abnormality	82.1 94.52	-----	-----	-----	-----	-----	-----

5.3. Sound-based DL techniques

Fraiwan et al. [65] designed and evaluated a technique that notes respiratory and lung diseases from lung sounds with the raw acoustic signal dataset using deep CNN and bidirectional LSTM units called (CNN+BDLSTM). The K fold cross-validation scheme trained the model. The advanced model achieved high levels of quality, such as sensitivity and specificity of 98.43% and 99.69%, which opens up new possibilities for using DL applications in clinical programs. Pham et al. [66] presented a robust deep-learning technique for classifying anomalies and detecting illnesses in respiratory cycles that depend on sound using an auscultation record. With a dataset used of ICBHI, the model was trained using a CNN-MOE architecture. According to the results shown in the Table 3.

Aykanat et al.[67] This research represented a significant advance in the use of the medical stethoscope by developing it into an electronic one. The electronic stethoscope, in turn, contains some programs that help transmit the sounds of the respiratory system to the computer, where the computer then analyzes and diagnoses these sounds using the previously stored sounds. When the network is trained with the help of CNN-based DL by utilizing the characteristics of the Mel-frequency cepstral coefficients (MFCC) mixed with those of the SVM, some good results were discovered are listed in the table 3. Hazra et al.[68] This study focuses on developing methods for using sounds produced by the respiratory system in the early detection of diseases (such as bronchiectasis, Pneumonia and chronic bronchiolitis).this is done after extracting the acoustic characteristics, and it is fed into a file for acoustic data, where it is categorized using 2D CNN. Owing to the lack of layers required in training the algorithm, this model obtained results with high accuracy.

Kumar et al.[69] The suggested system can categorize early patient COVID-19 disease based on gathered chest X-ray images and Coswara cough (sound) samples from possibly sick individuals. Cough samples recorded are subjected to a series of pre-processing steps that use speech signal processing methods. The MFCC characteristics are retrieved with the assistance of deep CNNs.

Table 3. Comparison of research using ultrasound-based DL techniques for lung disease detection

Ref/Year	Algorithm	Model	Type of diseases	Performance matrices						
				Accuracy (%)	**Sensitivity (%)**	**Specificity (%)**	**F1-score (%)**	**Precision (%)**	**ROC (%)**	**AUC (%)**
[66]/ 2021	CNN	CNN-MOE	classifying anomalies and detecting illnesses in respiratory cycles	-----	97.9	86.7	-----	82.4	-----	-----
[70]/ 2021	DNN	CNN, BDLSTM	lung diseases	-----	98.43	99.69	-----	-----	-----	-----
[67]/ 2017	CNN	MFCC SVM	Lung diseases	86 86	-----	-----	-----	-----	-----	-----
[68]/ 2021	2D CNN	MFCC	bronchiectasis, Pneumonia and chronic bronchiolitis	92.39	-----	-----	-----	-----	-----	-----
[69]/ 2022	CNN	MFCC	COVID-19	98.70	-----	-----	-----	-----	-----	-----

6. Performance Matrices

In this section, we will count the most prevalent measures in previous studies, such as sensitivity, specificity, accuracy, F1-score, precision, ROC, and AUC, which are all important metrics to measure in order to obtain the best model for lung diseases detections [71]. These performance metrics are commonly used to assess the impact of DL algorithms in diagnosing lung disorders. It is important to note that these metrics are not independent and can be influenced by various factors, including the size and quality of the dataset, the type of DL model used, and the specific application of the model. Therefore, it is essential to consider these metrics in conjunction with other factors.

A Confusion Matrix is a table with a specific shape that tabulates the algorithm's performance and efficiency based on its outcomes, with the actual values represented as rows in the matrix and the acceptable values displayed as columns and vice versa. The diagonally arranged values show the cases that are guessed correctly, while the others represent the wrong expectation, and the increase in the (diagonal) matrix values is better than the number of the lower values. Table 4 shows the Confusion Matrices cases. Table 4 represents positive or negative cases: TP, TN, FP, and FN are classified into two groups [72].

Table 4. Confusion Matrices cases

Parameters	Symbol	Description
True Positives	TP	Represent the positive observed and forecasted cases
True Negatives	TN	Represent the observed and forecasted negative cases
False Positives	FP	Occurred when actual instances were negative and anticipated cases were positive
False Negatives	FN	Occurred when actual instances were positive while anticipated cases were negative

Accuracy can be found by dividing all collected samples' true positive and negative cases.

$$Accuracy=\frac{TP+TN}{TN+TP+FN+FP} \tag{1}$$

Sensitivity is determined by separating into equal parts the positive case forecasted correctly, the positive case appropriately forecasted, and the negative case forecasted improperly. This feature is useful. This statistic is helpful when an FN is further of a problem than an FP.

$$Sensitivity = \frac{TP}{FN+TP} \tag{2}$$

Specificity represents the capacity of the framework to detect negative instances accurately, and once all negative samples have been discovered, the model is good since it provides no unexpected outcomes.

$$Specificity = \frac{TN}{FP+TN} \tag{3}$$

Precision is calculated by dividing the number of true positive cases by the total number of positive cases that were predicted, including both correctly and falsely predicted positive cases. When an FP is more concerning than an FN, it is a helpful metric.

$$Precision = \frac{TP}{TP+FP} \tag{4}$$

F1 score, while attempting to improve the model's accuracy, the sensitivity decreases. This metric may be viewed as a corresponding mean of accuracy and sensitivity, providing a comprehensive portrayal among both measures, with an F1 score reaching its highest rate at one and its poorest value at zero.

$$F1\ score = 2\times \frac{(Precision\times sensitivity)}{(Precision\times sensitivity)} \tag{5}$$

The receiver operator characteristic curve (ROC) is a rating metric for the binary classification task. At various threshold values, it shows the True-Positive Rate versus the False-Positive Rate [73].

The likelihood ratio (ROC) curve measures how effectively the equation separates two variables. Two-dimensional AUC measures the ROC curve area. This reflects model performance higher AUC.

$$TPR = \frac{TP}{TP+FN} \tag{6}$$

$$FPR = \frac{FP}{FP+TN} \tag{7}$$

7. Advantages and Challenges

7.1. Advantages of DL algorithm for lung diseases diagnosis

CNNs, DNNs, and GANs are DL models with advantages in diagnosing lung diseases based on medical imaging techniques such as X-rays and CT. The choice of an algorithm may depend on the specific application and the available data, and different algorithms may be more appropriate for different types of lung diseases or different imaging modalities. Here are some advantages of each type of network:

CNNs advantages

- CNNs are specifically designed for image analysis tasks and are therefore well-suited for processing medical imaging data [74].
- They can learn and identify complex features in medical images, making them helpful in identifying patterns and characteristics associated with different lung diseases[75].
- CNNs can handle large amounts of data and can be trained with relatively small amounts of labelled data [76].

DNNs advantages

- DNNs are more general-purpose models that can be applied to various medical imaging tasks, including lung disease diagnosis [77].
- They can learn complex nonlinear relationships between input data and output labels, making them well-suited for identifying subtle patterns and features in medical images [78].
- DNNs can build more complex models than CNNs, improving lung disease diagnosis accuracy [79].

GANs advantages

- GANs can be used to generate synthetic medical images, which can be used to augment existing datasets or to generate images with specific features or characteristics [80].
- GANs can generate medical images that simulate different lung diseases or imaging modalities, such as X-rays and CT[81].
- GANs can be used in conjunction with CNNs or DNNs to enhance the accuracy of lung disease identification by providing additional training data or generating more informative features [82].

7.2. Challenges and limitations for lung diseases diagnosis

DL has *shown* great promise in medical image analysis and has demonstrated high accuracy in diagnosing various diseases, including lung diseases. However, lung disease diagnosis based on DL still has several challenges and limitations. Some of these challenges and limitations are:

- Insufficient data: One of the significant challenges is the availability of labelled data, especially for rare or complex diseases. These networks require large amounts of high-quality data to learn from; without enough data, their performance can be limited [83].
- Overfitting: Another challenge is overfitting when the model grasps to distinguish distinct features to the training dataset but is not generalizable to new data. This can result in poor performance on new or unseen data [84].

- Interpretability: While DL models have shown excellent performance in many applications, the interpretability of these models can be challenging. It can be difficult to understand how the model arrived at its decision, which is vital for gaining the trust and acceptance of medical professionals [85].
- Variability in medical images: Medical images can be highly variable, and the quality of the images can vary based on factors such as the imaging modality, the imaging device, and the patient's position. This variability can make it difficult for deep-learning models to diagnose lung diseases accurately [86].
- Data imbalance: Imbalanced datasets, where significantly more examples of one class than another, can challenge DL models. This can result in biased models towards the majority class and may not perform well on the minority class [87].
- Generalization: DL models sometimes have difficulty generalizing to new or unseen data. This is especially problematic in the medical field, where new and rare diseases may not have enough labelled data to train a model with high accuracy [88].

Overcoming these challenges will require continued research and development of new techniques and models that can improve the accuracy and interpretability of these models.

8. Conclusion

Analysis of medical images is a complex and growing topic that needs many studies. One of the most critical problems facing researchers in DL research is the accurate diagnosis of medical images. Therefore, the paper provides a review to present the medical image analysis techniques of respiratory diseases, representing pneumonia, TB, lung cancer, and Covid-19. According to the statistics provided by the World Health Organization, it was found that Covid-19 and Pneumonia have the highest rates among other diseases. DL and image processing have great potential for diagnosing and treating lung diseases. By leveraging large amounts of medical data, DL algorithms can analyze lung images and detect patterns not visible to the naked eye. It can lead to earlier detection of lung diseases, more accurate diagnosis, and personalized treatment plans. To classify the four diseases, the researchers used different DL models, most notably VGGNet, ResNet, and Xception, significantly in research to overcome this problem. Good results were shown, as mentioned in Table 1, Table 2, and Table 3. It was noted that choosing CNN models is the most common in diagnosing medical images. X-ray, CT, and sound. This review recommends using Fetcher extraction with an image processing technique to generate images from the original image to train the network. In addition, this review mentioned the advantages and disadvantages of each type of DL model (CNN, DNN, GANs). Finally, this review explains lung disease detection's current challenges and limitations. Overall, DL and image processing offer exciting possibilities for improving the detection and treatment of lung diseases. Ongoing research in this field will continue to refine these techniques and explore new applications for this powerful technology.

Acknowledgements

The authors would like to thank the staff of the Department of Medical Instrumentation Engineering Techniques, Electrical Engineering Technical College, Middle Technical University-Baghdad, Iraq, for their support during this study.

References

[1] Forum of International Respiratory Societies. The Global Impact of Respiratory Disease, 2nd ed.; European Respiratory Society, Sheffield, UK, 2017; pp. 5–42.

[2] M. M. Rahaman et al., "Identification of COVID-19 samples from chest X-Ray images using deep learning: A comparison of transfer learning approaches," J Xray Sci Technol, vol. 28, no. 5, pp. 821-839, 2020, doi: 10.3233/XST-200715.

[3] R. Loddenkemper, G. Gibson, and Y. Sibille, "The burden of lung disease in Europe: why a European White Book on lung disease?," vol. 22, ed: Eur Respiratory Soc, 2003, pp. 869-69.doi: 10.1183/09031936.03.00107803

[4] O. E. Amani Yahiaoui and N. Yumusak, "A new method of automatic recognition for tuberculosis disease diagnosis using support vector machines," Biomedical Research, vol. 28, no. 9, pp. 4208-4212, 2017.

[5] A. A. A. Setio et al., "Validation, comparison, and combination of algorithms for automatic detection of pulmonary nodules in computed tomography images: The LUNA16 challenge," Med Image Anal, vol. 42, pp. 1-13, Dec 2017, doi: 10.1016/j.media.2017.06.015.

[6] C. Wu, C. Luo, N. Xiong, W. Zhang, and T.-H. Kim, "A Greedy Deep Learning Method for Medical Disease Analysis," IEEE Access, vol. 6, pp. 20021-20030, 2018, doi: 10.1109/access.2018.2823979.

[7] S. Hu et al., "Weakly supervised deep learning for covid-19 infection detection and classification from ct images," IEEE Access, vol. 8, pp. 118869-118883, 2020.doi: 10.1109/ACCESS.2020.3005510.

[8] C. C. Veghes, "The State of Artificial Intelligence in Medical Imaging," 2021.

[9] Y. Zhang, J. M. Gorriz, and Z. Dong, "Deep learning in medical image analysis," vol. 7, ed: MDPI, 2021, p. 74.doi: https://doi.org/10.3390/app11041675

[10] A. A. Mukhlif, B. Al-Khateeb, and M. Mohammed, "Classification of breast cancer images using new transfer learning techniques," Iraqi Journal For Computer Science and Mathematics, vol. 4, no. 1, pp. 167-180, 2023.doi: https://doi.org/10.52866/ijcsm.2023.01.01.0014

[11] A. S. Lundervold and A. Lundervold, "An overview of deep learning in medical imaging focusing on MRI," Zeitschrift für Medizinische Physik, vol. 29, no. 2, pp. 102-127, 2019.doi: https://doi.org/10.1016/j.zemedi.2018.11.002

[12] L. Alzubaidi et al., "Novel transfer learning approach for medical imaging with limited labeled data," Cancers, vol. 13, no. 7, p. 1590, 2021.doi: https://doi.org/10.3390/cancers13071590

[13] A. N. Zghair, "Assessment of Haematological Parameters in Drug-Resistant TB," Journal of Techniques, vol. 5, no. 1, pp. 137-143, 2023.doi: , doi: https://doi.org/10.51173/jt.v5i1.1082

[14] P. Van Dyck, F. Vanhoenacker, P. Van den Brande, and A. De Schepper, "Imaging of pulmonary tuberculosis," European radiology, vol. 13, pp. 1771-1785, 2003. doi:https://doi.org/10.1007/s00330-002-1612-y

[15] A. Khatri, R. Jain, H. Vashista, N. Mittal, P. Ranjan, and R. Janardhanan, "Pneumonia identification in chest X-ray images using EMD," in Trends in Communication, Cloud, and Big Data: Proceedings of 3rd National Conference on CCB, 2018, 2020: Springer, pp. 87-98. doi: 10.1007/978-981-15-1624-5_9

[16] E. Ayan and H. M. Ünver, "Diagnosis of pneumonia from chest X-ray images using deep learning," in 2019 Scientific Meeting on Electrical-Electronics & Biomedical Engineering and Computer Science (EBBT), 2019: Ieee, pp. 1-5. doi: 10.1109/EBBT.2019.8741582
[17] A. C. Borczuk, "Benign tumors and tumorlike conditions of the lung," Archives of pathology & laboratory medicine, vol. 132, no. 7, pp. 1133-1148, 2008.doi: https://doi.org/10.3390/jimaging6120131
[18] Q. Song, L. Zhao, X. Luo, and X. Dou, "Using deep learning for classification of lung nodules on computed tomography images," Journal of healthcare engineering, vol. 2017, 2017.doi: https://doi.org/10.1155/2017/8314740
[19] A. Webb, Introduction to biomedical imaging. John Wiley & Sons, 2022.
[20] K.-H. Ng and M. M. Rehani, "X ray imaging goes digital," vol. 333, ed: British Medical Journal Publishing Group, 2006, pp. 765-766.doi: 10.1136/bmj.38977.669769.2C
[21] D. S. Kermany et al., "Identifying medical diagnoses and treatable diseases by image-based deep learning," cell, vol. 172, no. 5, pp. 1122-1131. e9, 2018.doi: https://doi.org/10.1016/j.cell.2018.02.010
[22] M. G. F. Costa, C. F. Costa Filho, A. Kimura, P. C. Levy, C. M. Xavier, and L. Fujimoto, "A sputum smear microscopy image database for automatic bacilli detection in conventional microscopy," in 2014 36th Annual International Conference of the IEEE Engineering in Medicine and Biology Society, 2014: IEEE, pp. 2841-2844. doi: 10.1109/EMBC.2014.6944215
[23] X. Wang, Y. Peng, L. Lu, Z. Lu, M. Bagheri, and R. M. Summers, "Chestx-ray8: Hospital-scale chest x-ray database and benchmarks on weakly-supervised classification and localization of common thorax diseases," in Proceedings of the IEEE conference on computer vision and pattern recognition, 2017, pp. 2097-2106. doi: https://www.cc.nih.gov/drd/summers.html
[24] M. E. Chowdhury et al., "Can AI help in screening viral and COVID-19 pneumonia?," Ieee Access, vol. 8, pp. 132665-132676, 2020.doi: 10.1109/ACCESS.2020.3010287
[25] G. T. Herman, Fundamentals of computerized tomography: image reconstruction from projections. Springer Science & Business Media, 2009.doi: https://link.springer.com/book/10.1007/978-1-84628-723-7
[26] J. Shiraishi et al., "Development of a digital image database for chest radiographs with and without a lung nodule: receiver operating characteristic analysis of radiologists' detection of pulmonary nodules," American Journal of Roentgenology, vol. 174, no. 1, pp. 71-74, 2000.doi: 10.2214/ajr.174.1.1740071
[27] Y. D. Cid, V. Liauchuk, D. Klimuk, A. Tarasau, V. Kovalev, and H. Müller, "Overview of ImageCLEFtuberculosis 2019-Automatic CT-based Report Generation and Tuberculosis Severity Assessment," in CLEF (Working Notes), 2019.
[28] S. Diciotti, S. Lombardo, M. Falchini, G. Picozzi, and M. Mascalchi, "Automated segmentation refinement of small lung nodules in CT scans by local shape analysis," IEEE Transactions on Biomedical Engineering, vol. 58, no. 12, pp. 3418-3428, 2011.doi: 10.1109/TBME.2011.2167621.
[29] J. P. Cohen, P. Morrison, L. Dao, K. Roth, T. Q. Duong, and M. Ghassemi, "Covid-19 image data collection: Prospective predictions are the future," arXiv preprint arXiv:2006.11988, 2020.doi: https://doi.org/10.48550/arXiv.2006.11988.
[30] E. Al Hadhrami, M. Al Mufti, B. Taha, and N. Werghi, "Transfer learning with convolutional neural networks for moving target classification with micro-Doppler radar spectrograms," in 2018 International Conference on Artificial Intelligence and Big Data (ICAIBD), 2018: IEEE, pp. 148-154. doi: 10.1109/ICAIBD.2018.8396184
[31] O. Sevli, "A deep convolutional neural network-based pigmented skin lesion classification application and experts evaluation," Neural Computing and Applications, vol. 33, no. 18, pp. 12039-12050, 2021.doi: https://doi.org/10.1007/s00521-021-05929-4
[32] K. Simonyan and A. Zisserman, "Very deep convolutional networks for large-scale image recognition," arXiv preprint arXiv:1409.1556, 2014.doi: https://doi.org/10.48550/arXiv.1409.1556.
[33] H. Janoria, J. Minj, and P. Patre, "Classification of skin disease from skin images using transfer learning technique," in 2020 4th International Conference on Electronics, Communication and Aerospace Technology (ICECA), 2020: IEEE, pp. 888-895. doi: 10.1109/ICECA49313.2020.9297567.
[34] H. Qassim, A. Verma, and D. Feinzimer, "Compressed residual-VGG16 CNN model for big data places image recognition," in 2018 IEEE 8th annual computing and communication workshop and conference (CCWC), 2018: IEEE, pp. 169-175. doi: 10.1109/CCWC.2018.8301729.
[35] F. Chollet, "Xception: Deep learning with depthwise separable convolutions," in Proceedings of the IEEE conference on computer vision and pattern recognition, 2017, pp. 1251-1258. doi: 10.1109/CVPR.2017.195.
[36] M. M. A. Shibly, T. A. Tisha, T. A. Tani, and S. Ripon, "Convolutional neural network-based ensemble methods to recognize Bangla handwritten character," PeerJ Computer Science, vol. 7, p. e565, 2021.doi: https://doi.org/10.7717/peerj-cs.565.
[37] P. Gifani, A. Shalbaf, and M. Vafaeezadeh, "Automated detection of COVID-19 using ensemble of transfer learning with deep convolutional neural network based on CT scans," International journal of computer assisted radiology and surgery, vol. 16, pp. 115-123, 2021.doi: https://doi.org/10.1007/s11548-020-02286-w.
[38] Y. Zou, L. Zhao, S. Qin, M. Pan, and Z. Li, "Ship target detection and identification based on SSD_MobilenetV2," in 2020 IEEE 5th Information Technology and Mechatronics Engineering Conference (ITOEC), 2020: IEEE, pp. 1676-1680. doi: 10.1109/ITOEC49072.2020.9141734.
[39] M. Sandler, A. Howard, M. Zhu, A. Zhmoginov, and L.-C. Chen, "Mobilenetv2: Inverted residuals and linear bottlenecks," in Proceedings of the IEEE conference on computer vision and pattern recognition, 2018, pp. 4510-4520.:https://openaccess.thecvf.com/content_cvpr_2018/papers/Sandler_MobileNetV2_Inverted_Residuals_CVPR_2018_paper.pdf.
[40] A. V. Ikechukwu, S. Murali, R. Deepu, and R. Shivamurthy, "ResNet-50 vs VGG-19 vs training from scratch: A comparative analysis of the segmentation and classification of Pneumonia from chest X-ray images," Global Transitions Proceedings, vol. 2, no. 2, pp. 375-381, 2021.doi: https://doi.org/10.1016/j.gltp.2021.08.027.
[41] S. Rajaraman et al., "A novel stacked generalization of models for improved TB detection in chest radiographs," in 2018 40th Annual International Conference of the IEEE Engineering in Medicine and Biology Society (EMBC), 2018: IEEE, pp. 718-721. doi: https://doi.org/10.1007/s00521-021-06177-2.
[42] G. Capizzi, G. L. Sciuto, C. Napoli, D. Połap, and M. Woźniak, "Small lung nodules detection based on fuzzy-logic and probabilistic neural network with bioinspired reinforcement learning," IEEE Transactions on Fuzzy Systems, vol. 28, no. 6, pp. 1178-1189, 2019.doi: 10.1109/TFUZZ.2019.2952831.
[43] T. K. K. Ho and J. Gwak, "Utilizing Knowledge Distillation in Deep Learning for Classification of Chest X-Ray Abnormalities," IEEE Access, vol. 8, pp. 160749-160761, 2020, doi: 10.1109/access.2020.3020802.

[44] R. R. N. Tobias et al., "CNN-based deep learning model for chest X-ray health classification using tensorflow," in 2020 RIVF International Conference on Computing and Communication Technologies (RIVF), 2020: IEEE, pp. 1-6. doi: 10.1109/RIVF48685.2020.9140733.
[45] S. Gite, A. Mishra, and K. Kotecha, "Enhanced lung image segmentation using deep learning," Neural Comput Appl, pp. 1-15, Jan 3 2022, doi: 10.1007/s00521-021-06719-8.
[46] Y. H. Bhosale and K. Sridhar Patnaik, "IoT Deployable Lightweight Deep Learning Application For COVID-19 Detection With Lung Diseases Using RaspberryPi," presented at the 2022 International Conference on IoT and Blockchain Technology (ICIBT), 2022.doi: 10.1109/ICIBT52874.2022.9807725.
[47] A. Khadidos, A. O. Khadidos, S. Kannan, Y. Natarajan, S. N. Mohanty, and G. Tsaramirsis, "Analysis of covid-19 infections on a ct image using deepsense model," Frontiers in public health, vol. 8, p. 599550, 2020.doi: https://doi.org/10.3389/fpubh.2020.599550.
[48] Z. Wang, H. Xu, and M. Sun, "Deep learning based nodule detection from pulmonary CT images," in 2017 10th International Symposium on Computational Intelligence and Design (ISCID), 2017, vol. 1: IEEE, pp. 370-373. doi: 10.1109/ISCID.2017.107.
[49] P. Yadav, N. Menon, V. Ravi, and S. Vishvanathan, "Lung-gans: Unsupervised representation learning for lung disease classification using chest ct and x-ray images," IEEE Transactions on Engineering Management, 2021.doi: 10.1109/TEM.2021.3103334,
[50] H. Tang, C. Zhang, and X. Xie, "Automatic pulmonary lobe segmentation using deep learning," in 2019 IEEE 16th international symposium on biomedical imaging (ISBI 2019), 2019: IEEE, pp. 1225-1228. doi: 10.1109/ISBI.2019.8759468.
[51] H. Hou, W. Lv, and Q. Tao, "Hospital, T., Company, JT, Ai, T," Hospital, T., Wuhan, T., & Hospital, 2020.
[52] A. A. Ardakani, A. R. Kanafi, U. R. Acharya, N. Khadem, and A. Mohammadi, "Application of deep learning technique to manage COVID-19 in routine clinical practice using CT images: Results of 10 convolutional neural networks," Computers in biology and medicine, vol. 121, p. 103795, 2020.doi: https://doi.org/10.1016/j.compbiomed.2020.103795.
[53] A. M. Hasan, M. M. Al-Jawad, H. A. Jalab, H. Shaiba, R. W. Ibrahim, and A. a. R. AL-Shamasneh, "Classification of Covid-19 coronavirus, pneumonia and healthy lungs in CT scans using Q-deformed entropy and deep learning features," Entropy, vol. 22, no. 5, p. 517, 2020.doi: https://doi.org/10.3390/e22050517.
[54] Y. Pathak, P. K. Shukla, A. Tiwari, S. Stalin, and S. Singh, "Deep transfer learning based classification model for COVID-19 disease," Irbm, 2020.doi: 10.1016/j.irbm.2020.05.003.
[55] T. Yan, P. K. Wong, H. Ren, H. Wang, J. Wang, and Y. Li, "Automatic distinction between COVID-19 and common pneumonia using multi-scale convolutional neural network on chest CT scans," Chaos, Solitons & Fractals, vol. 140, p. 110153, 2020.doi: 10.1016/j.chaos.2020.110153.
[56] C. Liu, X. Wang, C. Liu, Q. Sun, and W. Peng, "Differentiating novel coronavirus pneumonia from general pneumonia based on machine learning," Biomedical engineering online, vol. 19, no. 1, pp. 1-14, 2020.doi: https://doi.org/10.1186/s12938-020-00809-9.
[57] L. Li et al., "Artificial intelligence distinguishes COVID-19 from community acquired pneumonia on chest CT. Radiology," ed, 2020.doi: https://doi.org/10.1038/s41467-020-17971-2.
[58] S. Wang et al., "A deep learning algorithm using CT images to screen for Corona Virus Disease (COVID-19)," European radiology, vol. 31, no. 8, pp. 6096-6104, 2021. 10.1007/s00330-021-07715-1.
[59] T. A. U.-M. Sadoon and M. H. Ali, "Coronavirus 2019 (COVID-19) Detection Based on Deep Learning," Al-Nahrain Journal for Engineering Sciences, vol. 23, no. 4, pp. 408-415, 2020.doi: 10.1007/s42979-022-01464-8.
[60] M. Barstugan, U. Ozkaya, and S. Ozturk, "Coronavirus (covid-19) classification using ct images by machine learning methods," arXiv preprint arXiv:2003.09424, 2020.doi: https://doi.org/10.48550/arXiv.2003.09424.
[61] V. Shah, R. Keniya, A. Shridharani, M. Punjabi, J. Shah, and N. Mehendale, "Diagnosis of COVID-19 using CT scan images and deep learning techniques," Emergency radiology, vol. 28, no. 3, pp. 497-505, 2021.doi: https://doi.org/10.1007/s10140-020-01886-y.
[62] H. Panwar, P. Gupta, M. K. Siddiqui, R. Morales-Menendez, P. Bhardwaj, and V. Singh, "A deep learning and grad-CAM based color visualization approach for fast detection of COVID-19 cases using chest X-ray and CT-Scan images," Chaos, Solitons & Fractals, vol. 140, p. 110190, 2020.doi: 10.1016/j.chaos.2020.110190.
[63] L. N. Rohmah and A. Bustamam, "Improved classification of coronavirus disease (COVID-19) based on combination of texture features using CT scan and X-ray images," in 2020 3rd International Conference on Information and Communications Technology (ICOIACT), 2020: IEEE, pp. 105-109. doi: covidwho-1105152.
[64] X. Wang et al., "A weakly-supervised framework for COVID-19 classification and lesion localization from chest CT," IEEE transactions on medical imaging, vol. 39, no. 8, pp. 2615-2625, 2020.doi: 10.1016/j.bspc.2022.104099.
[65] M. Fraiwan, L. Fraiwan, M. Alkhodari, and O. Hassanin, "Recognition of pulmonary diseases from lung sounds using convolutional neural networks and long short-term memory," Journal of Ambient Intelligence and Humanized Computing, pp. 1-13, 2021.doi: https://doi.org/10.1007/s12652-021-03184-y.
[66] L. Pham, H. Phan, R. Palaniappan, A. Mertins, and I. McLoughlin, "CNN-MoE Based Framework for Classification of Respiratory Anomalies and Lung Disease Detection," IEEE J Biomed Health Inform, vol. 25, no. 8, pp. 2938-2947, Aug 2021, doi: 10.1109/JBHI.2021.3064237.
[67] M. Aykanat, Ö. Kılıç, B. Kurt, and S. Saryal, "Classification of lung sounds using convolutional neural networks," EURASIP Journal on Image and Video Processing, vol. 2017, no. 1, p. 65, 2017/09/11 2017, doi: 10.1186/s13640-017-0213-2.
[68] R. Hazra and S. Majhi, "Detecting respiratory diseases from recorded lung sounds by 2d cnn," in 2020 5th International Conference on Computing, Communication and Security (ICCCS), 2020: IEEE, pp. 1-6. doi: 10.1109/ICCCS49678.2020.9277101.
[69] S. Kumar et al., "Chest X ray and cough sample based deep learning framework for accurate diagnosis of COVID-19," Computers and Electrical Engineering, vol. 103, p. 108391, 2022.doi: https://doi.org/10.1016/j.compeleceng.2022.108391.
[70] M. Fraiwan, L. Fraiwan, M. Alkhodari, and O. Hassanin, "Recognition of pulmonary diseases from lung sounds using convolutional neural networks and long short-term memory," J Ambient Intell Humaniz Comput, vol. 13, no. 10, pp. 4759-4771, 2022, doi: 10.1007/s12652-021-03184-y.
[71] S. V. Stehman, "Selecting and interpreting measures of thematic classification accuracy," Remote sensing of Environment, vol. 62, no. 1, pp. 77-89, 1997.doi: https://doi.org/10.1016/S0034-4257(97)00083-7.
[72] A. A. Mukhlif, B. Al-Khateeb, and M. A. Mohammed, "An extensive review of state-of-the-art transfer learning techniques used in medical imaging: Open issues and challenges," Journal of Intelligent Systems, vol. 31, no. 1, pp. 1085-1111, 2022.doi: https://doi.org/10.1515/jisys-2022-0198.
[73] S. Wu, W.-C. Yau, T.-S. Ong, and S.-C. Chong, "Integrated churn prediction and customer segmentation framework for telco business,"

IEEE Access, vol. 9, pp. 62118-62136, 2021.doi: 10.1109/ACCESS.2021.3073776.
[74] B. Savelli, A. Bria, M. Molinara, C. Marrocco, and F. Tortorella, "A multi-context CNN ensemble for small lesion detection," Artificial Intelligence in Medicine, vol. 103, p. 101749, 2020.doi: https://doi.org/10.1016/j.artmed.2019.101749.
[75] A. Al-Ajlan and A. El Allali, "CNN-MGP: convolutional neural networks for metagenomics gene prediction," Interdisciplinary Sciences: Computational Life Sciences, vol. 11, pp. 628-635, 2019.doi: https://doi.org/10.1007/s12539-018-0313-4.
[76] G. An, M. Akiba, K. Omodaka, T. Nakazawa, and H. Yokota, "Hierarchical deep learning models using transfer learning for disease detection and classification based on small number of medical images," Scientific reports, vol. 11, no. 1, p. 4250, 2021.doi: https://doi.org/10.1038/s41598-021-83503-7.
[77] V. Taran, Y. Gordienko, O. Rokovyi, O. Alienin, Y. Kochura, and S. Stirenko, "Edge intelligence for medical applications under field conditions," in Advances in Artificial Systems for Logistics Engineering: Springer, 2022, pp. 71-80.doi: https://doi.org/10.1007/978-3-031-04809-8_6.
[78] K. A. Tran, O. Kondrashova, A. Bradley, E. D. Williams, J. V. Pearson, and N. Waddell, "Deep learning in cancer diagnosis, prognosis and treatment selection," Genome Medicine, vol. 13, no. 1, pp. 1-17, 2021.doi: https://doi.org/10.1186/s13073-021-00968-x.
[79] S. T. Ahmed and S. M. Kadhem, "Using Machine Learning via Deep Learning Algorithms to Diagnose the Lung Disease Based on Chest Imaging: A Survey," International Journal of Interactive Mobile Technologies, vol. 15, no. 16, 2021.doi: 10.3991/ijim.v15i16.24191.
[80] Q. Guan et al., "Medical image augmentation for lesion detection using a texture-constrained multichannel progressive GAN," Computers in Biology and Medicine, vol. 145, p. 105444, 2022.doi: https://doi.org/10.1016/j.compbiomed.2022.105444.
[81] F. Munawar, S. Azmat, T. Iqbal, C. Grönlund, and H. Ali, "Segmentation of lungs in chest X-ray image using generative adversarial networks," Ieee Access, vol. 8, pp. 153535-153545, 2020.doi: 10.1016/j.compbiomed.2022.105444
[82] M. Kim et al., "Deep learning in medical imaging," Neurospine, vol. 16, no. 4, p. 657, 2019.
[83] Y. Li and X. Chao, "Toward sustainability: trade-off between data quality and quantity in crop pest recognition," Frontiers in plant science, vol. 12, p. 2959, 2021.doi: 10.3389/fpls.2021.811241.
[84] T. Han, Y.-F. Li, and M. Qian, "A hybrid generalization network for intelligent fault diagnosis of rotating machinery under unseen working conditions," IEEE Transactions on Instrumentation and Measurement, vol. 70, pp. 1-11, 2021.doi: https://doi.org/10.1007/s11465-021-0652-4.
[85] R. ElShawi, Y. Sherif, M. Al-Mallah, and S. Sakr, "Interpretability in healthcare: A comparative study of local machine learning interpretability techniques," Computational Intelligence, vol. 37, no. 4, pp. 1633-1650, 2021.doi: 10.1111/coin.12410.
[86] F. Renard, S. Guedria, N. D. Palma, and N. Vuillerme, "Variability and reproducibility in deep learning for medical image segmentation," Scientific Reports, vol. 10, no. 1, pp. 1-16, 2020.doi: https://doi.org/10.1038/s41598-020-69920-0.
[87] L. Gao, L. Zhang, C. Liu, and S. Wu, "Handling imbalanced medical image data: A deep-learning-based one-class classification approach," Artificial intelligence in medicine, vol. 108, p. 101935, 2020.doi: https://doi.org/10.1016/j.artmed.2020.101935.
[88] Y. Bengio, A. Lodi, and A. Prouvost, "Machine learning for combinatorial optimization: a methodological tour d'horizon," European Journal of Operational Research, vol. 290, no. 2, pp. 405-421, 2021.doi: https://doi.org/10.1016/j.ejor.2020.07.063.